Physics Letters A 372 (2008) 4943–4946

Contents lists available at ScienceDirect

Physics Letters A

www.elsevier.com/locate/pla

The influence of interband tunneling on leakage current in manganite/titanate heterojunction

Peng Han [a,b,*], Jin-Feng Jia [a]

[a] Department of Physics, Tsinghua University, Beijing 100084, China
[b] Institute of Physics, Chinese Academy of Sciences, Beijing 100190, China

ARTICLE INFO

Article history:
Received 23 February 2008
Accepted 15 May 2008
Available online 20 May 2008
Communicated by R. Wu

PACS:
73.40.Lq
77.84.Dy
72.20.-i

Keywords:
Perovskite oxide
Heterojunction
Leakage current

ABSTRACT

The behavior of leakage current at reverse bias in p-$La_{0.9}Sr_{0.1}MnO_3$/n-$SrNb_{0.01}Ti_{0.99}O_3$ heterojunction has been theoretically studied by calculating interband tunneling current with various doping densities and temperatures. Our results reveal that the reduction of leakage current with decrease of doping density and increase of temperature originates from properties of interband tunneling.

1. Introduction

The novel physics properties of colossal magnetoresistance, ferromagnetism, ferroelectricity, and photoelectricity in the perovskite oxide materials provide great potential applications for these correlated electron systems. To realize the practical application of the perovskite oxide materials, many investigations have been performed on the low-dimensional perovskite oxide devices. Recently, the all-oxide and oxide–silicon p–n junctions, p–i–n junctions, and tunneling junctions with good rectifying property have been fabricated by many groups [1–13]. Besides the experimental efforts, the transport mechanism of the oxide p–n junctions also has been studied from theoretical aspects [14–17]. As indicated in Ref. [14], the conventional semiconductor theory for p–n junction can be phenomenologically employed to analyze the carrier distribution, the electric field intensity, the band structure, and the I–V characteristics of the multi-correlated perovskite oxide heterojunction. Based on this hypothesis, the good agreement between theoretical and experimental I–V characteristics of perovskite oxide p–n junction with forward and reverse bias has been obtained [15,17]. However, all these theoretical research works [14–17] are focused on the I–V characteristics above 190 K and few theoretical study about the transport process below 190 K has been reported. Especially, the theoretical study on the behaviors of leakage current at reverse bias in the perovskite p–n junction with low temperature is still empty.

As shown in our previous work [17], the trap assisted tunneling process caused by the oxygen vacancy induced states has been proven as the dominant mechanism for the leakage current in the manganite/titanate p–n junction with low reverse bias. In addition, it also has been revealed that the interband tunneling process plays an important role for the leakage current with high reverse bias. However, as indicated in Ref. [18], the density of trap centers for the trap assisted tunneling process decreases with the increase of temperature and the intensity of trap assisted tunneling current decreases. Thus, the effect of direct interband tunneling between the valence band of p side and the conduction band of n side on the leakage current cannot be omitted anymore with low reverse bias at low temperature.

In this work, we present the theoretical study on the behavior of leakage current with reverse bias based on the calculation of interband tunneling current in $La_{0.9}Sr_{0.1}MnO_3$/$SrNb_{0.01}Ti_{0.99}O_3$ (LSMO/SNTO) heterojunction at low temperature. The energy band and the tunneling barrier, which are used in the calculation, are obtained self-consistently by solving the Poisson equation and drift–diffusion formulas. The good agreement between the calculated results and the experimental data reveals that the decrease

* Corresponding author at: Department of Physics, Tsinghua University, Beijing 100084, China. Tel./fax: +86 10 82649299.
E-mail address: hanpeng@aphy.iphy.ac.cn (P. Han).

0375-9601/$ – see front matter
doi:10.1016/j.physleta.2008.05.033

of leakage current with the increase of temperature at T below 130 K originates from the property of interband tunneling. In addition, it has been revealed that the leakage current decreases with the decrease of doping density in LSMO due to the increase of barrier width for interband tunneling.

2. Theoretical model

The behavior of the electrostatic potential $\phi(x)$, the energy band, the electric field intensity $E(x)$, the concentrations of electron $n(x)$ and hole $p(x)$ under the external bias voltage V_{bias} in the LSMO/SNTO heterojunction are obtained self-consistently by solving the Poisson equation, electron and hole continuity equations on the basis of drift–diffusion model. And the Richardson thermionic emission current is taking into account as the interface condition to treat the current across the interface of heterojunction. The formulas, the boundary conditions, and the detailed arithmetic can be seen in Refs. [15] and [19,20].

With the forward bias voltage, the drift–diffusion current dominates the transport process of p–n junctions. However, the mobile electrons and holes have essentially been swept out of the space charge region and the drift–diffusion current can be neglected with the reverse bias. For this case, the bottom of the conduction band of n region decreases with the increase of reverse bias. Thus, electrons in the valence band on the p side can directly tunnel into the empty states in the n side with energy between E_{vp} and E_{fn}, where E_{vp} is the top of the valence band in the homogeneous region of the p side and E_{fn} is the Fermi level in the homogeneous region of the n side. The interband tunneling current is written as [21,22]

$$J = q\int_{E_{fn}}^{E_{vp}} N(E)f(E)T(E)\,dE \tag{1}$$

with tunneling rate $T(E) = \frac{\hbar}{\sqrt{2m_c^* E}}\Im[\psi_E^*(x)\frac{d}{dx}\psi_E(x)]$, where q represents the electric charge, "$\Im$" denotes the imaginary part of a complex number, m_c^* is the electron effective mass, and $\psi_E(x)$ is the wave function obtained by solving the Schrödinger equation [23]. $N(E)$ is the density of state and $f(E)$ is the Fermi distribution function, respectively.

3. Results and discussion

The energy band, the electric field intensity, and the distribution of carrier density are calculated self-consistently based on the Poisson equation and the drift–diffusion formulas [15,19] with concentrations of the acceptor and the donor are $N_a = 4.0\times10^{19}$ cm^{-3} and $N_d = 2.0\times10^{20}$ cm^{-3} at $T = 90$ and 130 K, respectively. The other necessary parameters used in the calculation are given in Table 1, and the effect of temperature on the carrier mobility and dielectric constant [24–26] has been taken into account in our calculation.

Fig. 1 presents the energy band of LSMO/SNTO heterojunction under -1.0 V bias voltage at $T = 130$ K with $N_a = 2.0\times10^{19}$ cm^{-3} (solid line) and 4.0×10^{19} cm^{-3} (dashed line), respectively, and the donor concentration is $N_d = 2.0\times10^{20}$ cm^{-3}. In this figure, the diagrams of energy band show that the space charge region of LSMO decreases and the barrier width between the valence band of p side and the conduction band of n side decreases with the increase of acceptor concentration. Additionally, the distributions of electric field intensity with 0.0 V bias (solid curve), 0.8 V bias (dashed curve), and -0.8 V (dotted curve) are presented in Fig. 2, respectively. As indicated in this figure, the electric field intensity increases with the applied reverse bias and decreases with the forward bias. Furthermore, the distributions of carrier densities at

Table 1
Material parameters used in the calculation [14,26–28]

Parameters	LSMO	SNTO
Band gap E_g (eV)	1.0	3.0
Affinity energy χ (eV)	3.95	4.05
Dielectric constant ε (ε_0)	10.0	300.0
Electron mobility μ_n (cm^2/V s)	10.0	8.0
Hole mobility μ_p (cm^2/V s)	1.8	0.1

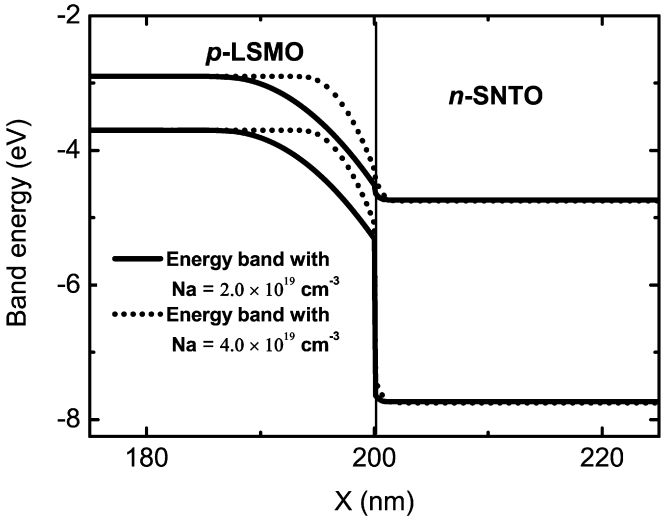

Fig. 1. The band energy of the $La_{0.9}Sr_{0.1}MnO_3/SrNb_{0.01}Ti_{0.99}O_3$ heterojunction with -1.0 V bias at $T = 130$ K with concentration of acceptor N_a as 2.0×10^{19} cm^{-3} (solid line), and 4.0×10^{19} cm^{-3} (dotted line), respectively. The concentration of donor $N_d = 2.0\times10^{20}$ cm^{-3}.

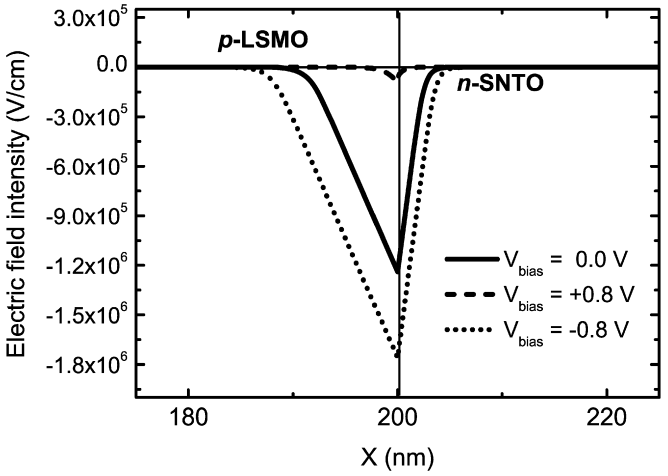

Fig. 2. The distribution of electric field intensity at $T = 130$ K with bias voltage as 0.8 V (dashed line), 0.0 V (solid line), and -0.8 V (dotted line), respectively.

$T = 90$ K and 130 K are plotted in Fig. 3, respectively. The comparison between the carrier densities at $T = 90$ K and 130 K shows that the concentrations of minority carrier (electrons in p region and holes in n region) decrease with the decrease of temperature.

The theoretical I–V characteristics with reverse bias are obtained by solving Eq. (1) and the forward I–V curves are calculated with the Poisson equation and the drift–diffusion formulas [15,19], respectively. Combining with the experimental data obtained from Ref. [29], the comparison between the calculated and measured I–V curves with $T = 90$ and 130 K are given in Fig. 4, respectively. As shown in this figure, the leakage current increases monotonically and rapidly with the increase of reverse bias, and decreases with the increase of temperature. The good agreement between

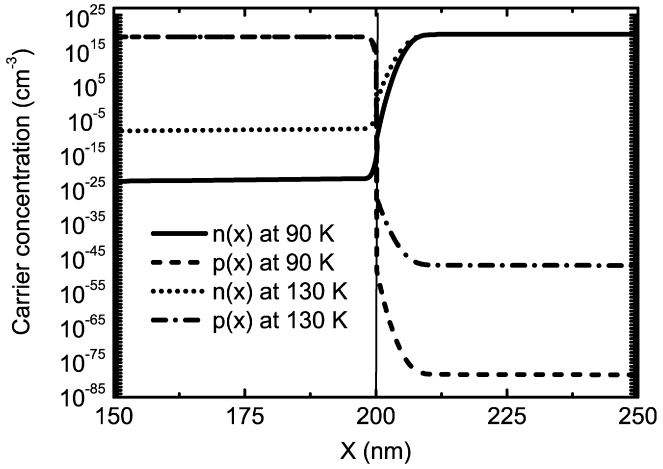

Fig. 3. The distribution of carrier densities in the $La_{0.9}Sr_{0.1}MnO_3/SrNb_{0.01}Ti_{0.99}O_3$ heterojunction with 0.0 V bias voltage at $T = 90$ K and 130 K, respectively.

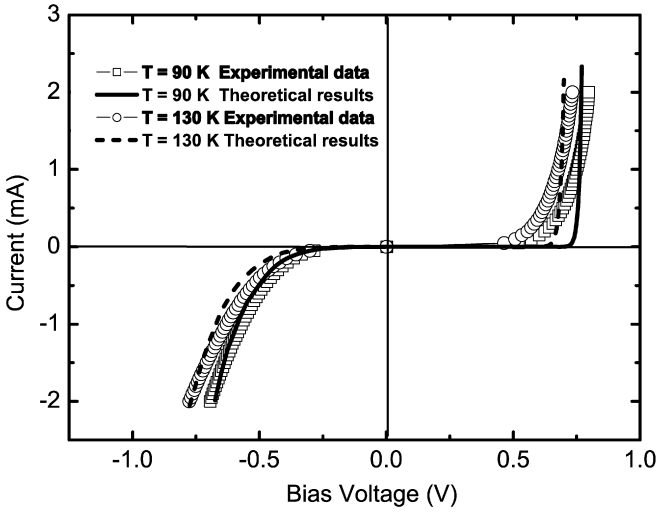

Fig. 4. The theoretical and experimental I–V curves with reverse and forward bias at $T = 90$ K and 130 K, respectively. The experimental data are obtained from Ref. [29].

theoretical and experimental I–V characteristics with reverse bias reveals that the behaviors of leakage current in the LSMO/SNTO heterojunction below $T = 130$ K originate from the properties of interband tunneling. The temperature dependent behavior of the leakage current can be explained with the theory of tunneling as follows. The Fermi distribution function of electrons in the valence band of p region $f(E) = \frac{1}{1+\exp(\frac{E-E_{fp}}{k_B T})}$, where E_{fp} describes the Fermi level of the homogeneous region of the p side and k_B is the Boltzmann's constant, decreases with the increase of temperature. And therefore, the intensity of tunneling current decreases with temperature according to Eq. (1).

In addition, to reveal the effect of doping density on the behavior of the leakage current, we plotted the calculated I–V curves of LSMO/SNTO heterojunction with $N_a = 2.0 \times 10^{19}$ cm^{-3} (solid curve), 4.0×10^{19} cm^{-3} (dotted curve), and 6.0×10^{19} cm^{-3} (dashed curve) in Fig. 5, respectively, and the donor concentration is $N_d = 2.0 \times 10^{20}$ cm^{-3}. As presented in this figure, the intensity of the leakage current increases with the increase of N_a, and this behavior is due to the decrease of barrier width for tunneling with the increase of doping density as illustrated in Fig. 1.

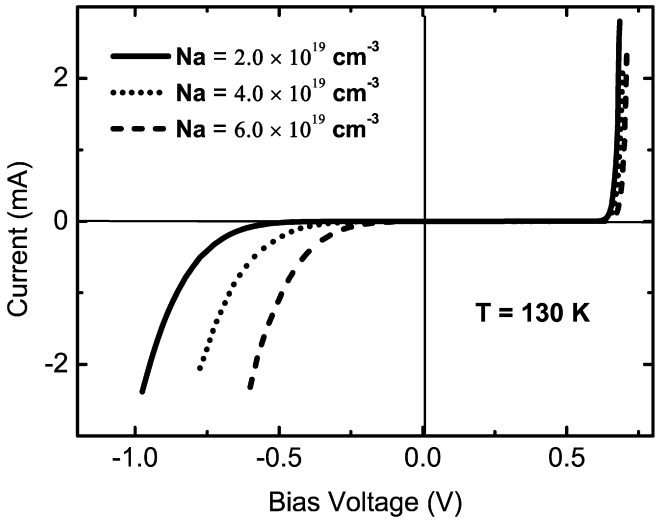

Fig. 5. The theoretical I–V characteristics with N_a as 2.0×10^{19} cm^{-3} (solid curve), 4.0×10^{19} cm^{-3} (dotted curve), and 6.0×10^{19} cm^{-3} (dashed curve), respectively. The concentration of donor $N_d = 2.0 \times 10^{20}$ cm^{-3}.

4. Summary

In summary, the behaviors of leakage current with reverse bias in the p-LSMO/n-SNTO heterojunction have been theoretically studied based on the calculation of interband tunneling current with various doping densities and temperatures. Our results reveal that the decrease of leakage current with the increase of temperature with T below 130 K is caused by the decrease of Fermi distribution function of electrons in the valence band of p region. In addition, the leakage current increases with the increase of the doping density due to the reduction of barrier width for interband tunneling. We hope these results will benefit to the further study of the oxide electronics in the future.

Acknowledgements

P.H. acknowledges Prof. K.-j. Jin for her helpful discussions. This work was supported by the National Natural Science Foundation of China, and the National Basic Research Program of China.

References

[1] M. Sugiura, K. Uragou, M. Tachiki, T. Kobayashi, J. Appl. Phys. 90 (2001) 187.
[2] C. Mitra, G. Köbernik, K. Dörr, K.-H. Müller, L. Schultz, P. Raychaydhuri, R. Pinto, E. Wieser, J. Appl. Phys. 91 (2002) 7715.
[3] C. Mitra, P. Raychaudhuri, K. Dörr, K.H. Müller, L. Schultz, P.M. Oppeneer, S. Wirth, Phys. Rev. Lett. 90 (2003) 017202.
[4] D. Hunter, K. Lord, T.M. Williams, K. Zhang, A.K. Pradhan, D.R. Sahu, J.-L. Huang, Appl. Phys. Lett. 89 (2006) 092102.
[5] L.M.B. Alldredge, R.V. Chopdekar, B.B. Nelson-Cheeseman, Y. Suzuki, Appl. Phys. Lett. 89 (2006) 182504.
[6] K.-j. Jin, H.B. Lu, Q.L. Zhou, K. Zhao, Z.H. Chen, B.L. Cheng, G.Z. Yang, Sci. Technol. Adv. Mater. 6 (2005) 833.
[7] K. Zhao, K.-J. Jin, H.B. Lu, Y.H. Huang, Q.L. Zhou, M. He, Z.H. Chen, Y.L. Zhou, G.Z. Yang, Appl. Phys. Lett. 88 (2006) 141914.
[8] K. Zhao, K.J. Jin, Y.H. Huang, S.Q. Zhao, H.B. Lu, M. He, Z.H. Chen, Y.L. Zhou, G.Z. Yang, Appl. Phys. Lett. 89 (2006) 173507.
[9] K. Zhao, K.J. Jin, Y.H. Huang, H.B. Lu, M. He, Z.H. Chen, Y.L. Zhou, G.Z. Yang, Physica B 373 (2006) 72.
[10] H.B. Lu, K.J. Jin, K. Zhao, Y.H. Huang, M. He, Z.H. Chen, Y.L. Zhou, G.Z. Yang, Adv. Sci. Technol. 45 (2006) 2582.
[11] K.-j. Jin, K. Zhao, H.B. Lu, L. Liao, G.Z. Yang, Appl. Phys. Lett. 91 (2007) 081906.
[12] G.Z. Liu, K.J. Jin, J. Qiu, M. He, H.B. Lu, J. Xing, Y.L. Zhou, G.Z. Yang, Appl. Phys. Lett. 91 (2007) 252110.
[13] T.F. Zhou, G. Li, N.Y. Wang, B.M. Wang, X.G. Li, Y. Chen, Appl. Phys. Lett. 88 (2006) 232508.
[14] K.-j. Jin, H.B. Lu, Q.L. Zhou, K. Zhao, B.L. Cheng, Z.H. Chen, Y.L. Zhou, G.Z. Yang, Phys. Rev. B 71 (2005) 184428.

[15] Q.L. Zhou, K.J. Jin, H.B. Lu, P. Han, Z.H. Chen, K. Zhao, Y.L. Zhou, G.Z. Yang, Europhys. Lett. 71 (2005) 283.
[16] J. Qiu, K.J. Jin, P. Han, H.B. Lu, C.L. Hu, B.P. Wang, G.Z. Yang, Europhys. Lett. 79 (2007) 57004.
[17] P. Han, K.J. Jin, H.B. Lu, Q.L. Zhou, Y.L. Zhou, G.Z. Yang, Appl. Phys. Lett. 91 (2007) 182102.
[18] E. Suzuki, D.K. Schroder, Y. Hayashi, J. Appl. Phys. 60 (1986) 3616.
[19] K. Horio, H. Yanai, IEEE Trans. Electron Devices 37 (1990) 1093.
[20] K. Yang, J.R. East, G.I. Haddad, Solid-State Electron. 36 (1993) 321.
[21] D.A. Neamen, Semiconductor Physics and Devices Basic Principles, third ed., McGraw–Hill, New York, 2003.
[22] S.M. Sez, Physics of Semiconductor Devices, Wiley, New York, 1981.
[23] O. Pinaud, J. Appl. Phys. 92 (2002) 1987.
[24] H.P.R. Ferderikse, W.R. Thurber, W.R. Hosler, Phys. Rev. 134 (1964) A442.
[25] G. Rupprecht, R.O. Bell, Phys. Rev. 135 (1964) A748.
[26] R. Moos, K.H. Härdtl, J. Appl. Phys. 80 (1996) 393.
[27] S. Myhajlenko, A. Bell, F. Ponce, J.L. Edwards Jr., Y. Wei, B. Craigo, D. Convey, H. Li, R. Liu, J. Kulik, J. Appl. Phys. 97 (2005) 014101.
[28] S. Chambers, Y. Liang, Z. Yu, R. Droopad, J. Ramdani, K. Eisenbeiser, Appl. Phys. Lett. 77 (2000) 1662.
[29] K.-j. Jin, H.B. Lu, Q.L. Zhou, K. Zhao, G.Z. Yang, J. Magn. Magn. Mater. 303 (2006) 329.